Energy-Filtered Scanning Tunneling Microscopy using a Semiconductor Tip

P. Sutter, P. Zahl, E. Sutter, and J. E. Bernard

Department of Physics, Colorado School of Mines, Golden, Colorado 80401
(Received 2 December 2002; published 24 April 2003)

The use of cleaved, [111]-oriented monocrystalline InAs probe tips enables state-specific imaging in constant-current filled-state scanning tunneling microscopy. On Si(111)-(7×7), the adatom or rest-atom dangling-bond states can thus be mapped selectively at different tip-sample bias. This state-selective imaging is made possible by energy gaps in the projected bulk band structure of the semiconductor probe. The lack of extended bulk states in these gaps gives rise to efficient energy filtering of the tunneling current, to which only sample states not aligned with a gap contribute significantly.

PACS numbers: 68.37.Ef, 73.20.–r

Scanning tunneling microscopy (STM) [1] has become a key technique for measurements at the atomic and molecular level [2]. Increasingly, STM is used not only for topographic imaging, but to obtain atom-resolved spectroscopic information on sample electronic structure [3], vibrational properties [4], and chemical activity [5]. Meanwhile, the original experimental setup in STM has remained remarkably unchanged. In particular, the role and nature of the probe tip, conventionally a sharpened polycrystalline metal wire, have hardly evolved at all. The predominant use of metal tips limits the potential of STM for spectroscopic imaging, giving poor control over the sample states that contribute to the tunneling current [6]. The mapping of a given occupied sample state, for instance, may be strongly hindered by this lack of control. Conventional filled-state STM invariably is most sensitive to states closest to the sample Fermi energy (ε_F). The tunneling barrier reduces contributions from deeper valence states far from ε_F [7], which are thus difficult to image in traditional STM with a metal probe. Here we introduce semiconductors as a novel class of tip materials that can overcome these limitations [8]. We observe that constant-current STM (cc-STM) with a cleaved [111]-oriented InAs probe allows energy-filtered imaging, in which only sample states within a narrow energy interval, tunable via the tip-sample bias, contribute to the tunneling current. Using this novel technique, we demonstrate the selective imaging of rest-atom dangling-bond states through overlapping, higher-lying adatom orbitals on Si(111)-(7×7).

To illustrate the possibilities for spectroscopic STM arising with monocrystalline semiconductor probes, we used InAs tips for bias-dependent cc-STM on Si(111)-(7×7). Experiments were performed in a home-built scanning tunneling microscope operating at room temperature in ultrahigh vacuum (UHV). Clean Si(111)-(7×7) surfaces were prepared in UHV following standard procedures [5]. Doped (*n*-type, $n = 2 \times 10^{18}$ cm^{-3}) InAs probes were produced by cleavage in air from a (001) oriented InAs wafer. A cleavage corner, defined by the intersection of two {110} cleavage planes with the (001)

surface, served as the STM tip. In contrast to the conventional polycrystalline metal tips, our monocrystalline InAs probes have a well-defined crystal orientation. As-cleaved tips were briefly heated in UHV and then mounted into the microscope with their [111] zone axis perpendicular to the sample surface [9].

We used Si(111)-(7×7) as a model sample surface with well-known properties. Its structural features are summarized in Fig. 1 [12]. The unit cell consists of two halves, one of which has a stacking fault in the second layer. The topmost atomic layer comprises 12 atoms per unit cell, which are referred to as center or corner adatoms. The second layer, about 1 Å lower [11], holds six rest atoms. Each of the adatoms and rest atoms has a single dangling bond. These dangling bonds are the primary source of tunneling current in STM on
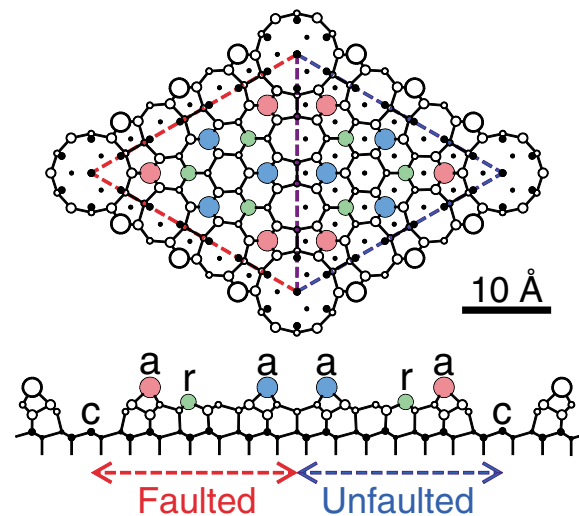

FIG. 1 (color). Si(111)-(7×7) structure [11]: Top view (top) and cross section (bottom). Atoms closest to the viewer are drawn largest. Twelve adatoms ("a"), among which are six corner and six center adatoms, constitute the topmost atomic layer. Rest atoms ("r") are located 1 Å below in the second layer. Corner-hole atoms ("c"), 4.4 Å below the adatom layer, mark the corners of the unit cell.

Si(111)-(7 × 7) [3]. The adatoms give rise to an occupied state 0.35 eV below ε_F. A second filled state, 0.8 eV below ε_F, is localized on the rest atoms. Si(111)-(7 × 7) thus represents a surface with two localized states at different energies, whose orbitals overlap considerably.

Conventional filled-state cc-STM is most sensitive to occupied states near the sample Fermi level [7]. On Si(111)-(7 × 7), it maps only the dangling bonds of the adatoms over a wide range of tip-sample bias, and is insensitive to the rest-atom state [13]. Filled-state images obtained with our cleaved InAs probes show a much richer bias dependence (Fig. 2). At low voltage [−1.0 V sample bias; Fig. 2(a)], sharp maxima in apparent height are localized at adatom positions, producing an image that closely matches those obtained with metal probes. With increasing negative voltage, however, these sharp maxima spread out to become shallower and elongated. At −1.7 V [Fig. 2(b)], the contrast maxima originally associated with the corner adatoms uniformly cover pairs of adjacent corner adatoms and rest atoms. Contrast from the center adatoms in the faulted half of the unit cell is spread into a ring of somewhat elevated apparent height, while having all but vanished in the unfaulted half. The shift of the maxima in apparent height continues to higher bias. At −2.0 V [Fig. 2(c)], the adatoms no longer appear to be protruding highest, but sharp and well-defined peaks are now located at the six rest-atom sites.

Figure 3 summarizes the bias dependence of the cc-STM contrast for sample voltages between −1.0 and −2.0 V, showing line profiles along the long diagonal of the (7 × 7) unit cell [10]. The profiles confirm a striking transition from pure adatom imaging at low bias to preferential rest-atom imaging at high bias. This transition involves a sharp drop in tunneling current from adatoms over a narrow bias range from −1.5 to −1.9 V. The tunneling resistances for corner adatoms and rest atoms become equal at −1.7 V in the unfaulted half, and at −1.8 V in the faulted half of the unit cell. Remarkably, the image obtained at the highest bias value, −2.0 V, maps the rest atoms about 0.5 Å above the corner adatoms, through the orbitals of the adatoms that lie 1 Å higher in the (7 × 7) structure [11]. Our images clearly cannot be interpreted as maps of sample topography, but instead constitute state-selective maps of individual dangling-bond orbitals at the Si(111)-(7 × 7) surface.

Figures 2 and 3 demonstrate a new mechanism of spectroscopic imaging in filled-state cc-STM with a semiconductor tip. In contrast to conventional cc-STM, STM with an InAs tip maps the energetically highest occupied state only at low bias, while a deeper valence state is selected for imaging by choosing a higher bias voltage. The repeatable observation of this effect with different InAs tips that likely have different configurations of the outermost tip atoms suggests a key role of bulk tip states in determining the tunneling current. For electrons tunneling from the sample surface into the tip at negative sample bias, current collection at the electrode attached to the tip requires that the transition into a localized state on the foremost tip atoms be followed by a second, energy-conserving transition into an extended bulk tip state [14]. Sample electrons that cannot make such a resonant transition are expected to contribute only weakly to the tunneling current. This need for a transfer into a bulk tip state can suppress the tunneling current in the case of a semiconductor probe, for example, if the
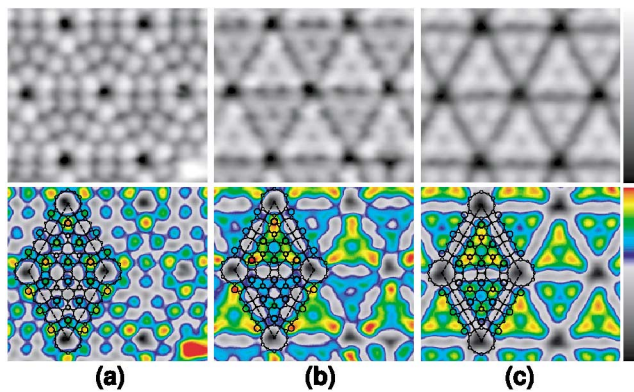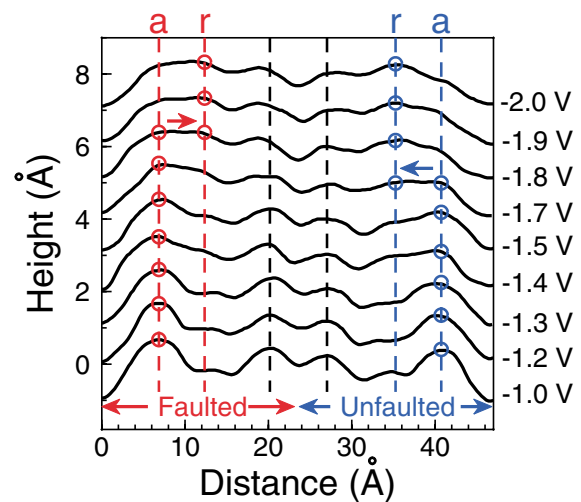

FIG. 2 (color). Constant-current STM images (top: gray scale; bottom: false color) of Si(111)-(7 × 7) obtained with a [111]-oriented InAs tip at different sample bias. (a) −1.0 V (height range: 1.8 Å); (b) −1.7 V (1.45 Å); and (c) −2.0 V (1.3 Å). The upper half of the unit cell is faulted. A simplified structure model of the (7 × 7) reconstruction is overlaid on one of the unit cells in each false color image. The gray and false-color scales used are shown next to column (c). Field of view: 60 Å × 67 Å; tunneling current: 300 pA.

FIG. 3 (color). STM line profiles between corner holes along the long diagonal of the (7 × 7) unit cell: Sample bias dependence between −1.0 and −2.0 V. Dashed lines mark corner adatom ("a") and rest atom ("r") positions on the diagonal in the two halves of the unit cell. Circles indicate the positions of maxima in apparent height in each profile.

final state falls into a band gap of the semiconductor [15]. This feature provides an opportunity to control tunneling from discrete sample states.

For tunneling into a polycrystalline metal tip, there is no gap in the density of final states [16]. A continuum of empty tip states above the Fermi energy implies a broad tunneling distribution, which for all bias voltages peaks at the sample Fermi level [7]. For samples with spatially overlapping dangling-bond orbitals at different energies, conventional STM with a metal tip preferentially maps the state closest to ε_F and is insensitive to the deeper valence orbitals. For a monocrystalline semiconductor STM tip, there may exist several gaps with vanishing density of states, as illustrated in Fig. 4(a). This panel shows the (111) surface-projected bulk band structure of InAs, matching the approximate orientation of our tips obtained by cleavage from a (001)-oriented wafer. It was calculated from first principles using local-density-functional theory with corrections for the band-gap discontinuity [17,18].

In addition to the fundamental band gap, which extends through the entire surface Brillouin zone (SBZ), there are several projected gaps. Most important here is the lowest projected gap in the conduction band, centered at Γ and persisting through about one third of the SBZ. At the zone center, the calculation shows the onset of this gap 1.92 eV above the valence band maximum, and a width $\varepsilon_p = 2.66$ eV.
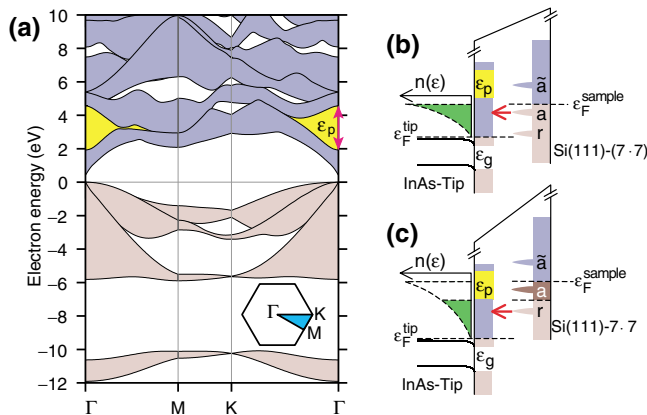

FIG. 4 (color). Tunneling into a [111]-oriented InAs tip: (a) Bulk bands of InAs projected onto the (111) surface Brillouin zone (inset). The zone-center width of the lowest projected gap in the conduction band is labeled ε_p. Energies are given with respect to the top of the valence band. (b), (c) Schematic band diagrams illustrating energy-filtered tunneling of electrons from a sample with two occupied surface states, such as Si(111)-(7 × 7), into a [111]-oriented InAs tip at negative sample bias. Sample surface states ("a", "ã", and "r") are indicated. The fundamental gap (ε_g) and the lowest (111)-projected gap (ε_p) of the InAs tip are shown, as is the schematic tunneling probability $n(\varepsilon)$ of electrons tunneling from sample to tip.

The absence of extended states in this projected gap can be expected to strongly affect the energy distribution of the tunneling current from sample to tip, as shown in Figs. 4(b) and 4(c). These panels give schematic band diagrams for electrons tunneling into an InAs tip from a sample [such as Si(111)-(7 × 7)] with two types of dangling-bond states, "a" and "r", at different energies. At low bias [Fig. 4(b)], the highest occupied surface state of the sample [the adatom state on Si(111)-(7 × 7)] falls below the projected tip gap. The tunneling distribution then resembles that for a metal tip; i.e., it is continuous with a peak at or near ε_F of the sample. With increasing bias, the highest valence state eventually lines up with the projected gap of the tip [Fig. 4(c)]. The vanishing projected tip density of states then strongly suppresses tunneling from this state, and a lower-lying state [the rest-atom state on Si(111)-(7 × 7)] dominates the tunneling current. Our band-structure calculation allows us to estimate the bias value at which the adatom surface state on Si(111)-(7 × 7) begins to line up with the projected conduction gap of our InAs probes. The predicted threshold for the transition from adatom to rest-atom imaging on Si(111)-(7 × 7) is −1.66 V, in excellent agreement with the transition observed in our experiments.

In the present case of an InAs probe, the (111)-projected conduction gap does not extend through the entire SBZ. The energy filter in an InAs tip may thus be transparent to tunneling electrons with large in-plane wave vector ($k_\parallel$). The $k_\parallel$ distribution in STM, however, is known to peak at $k_\parallel = 0$ [24]. We can estimate the width of the distribution from Heisenberg's uncertainty principle. Assuming an uncertainty $\Delta x \approx 2$ Å of the in-plane position of tunneling electrons, we find $\Delta k_\parallel \approx 1/2\Delta x \approx 0.25$ Å^{-1}, considerably smaller than the extent of the (111) projected gap in InAs (0.35 Å^{-1}). For a $k_\parallel$ distribution of this width, over 90% of the tunneling electrons have values of $k_\parallel$ below 0.35 Å^{-1}. An energy-filtering InAs probe should thus suppress tunneling from sample states tuned near the center of the projected gap with high efficiency, as is indeed observed in our experiments. A gradual reduction of adatom tunneling signal for applied bias above 1.7 V, as seen in Fig. 3, is expected due to the gradual expansion of the projected gap in k space and the finite width of the $k_\parallel$ distribution, of which an increasing fraction is blocked from tunneling with increasing bias.

Our observations suggest that a semiconductor such as InAs, used as a probe tip in STM, can serve as an energy filter with a narrow "pass band" between the fundamental gap (ε_g) and a projected conduction gap (ε_p). STM using such a probe offers exciting possibilities for spectroscopic imaging. If a sample has different dangling bonds with spatially overlapping orbitals, energy-filtered (EF) STM can selectively map each of these orbitals individually. In the more common case of spatially separated dangling bonds, EF-STM will provide contrast

between occupied states at different energies. If, for instance, different atomic species at the surface give rise to dangling bonds at different energies, EF-STM will be able to distinguish between these species. We thus foresee the ability to determine the local surface composition of semiconductor alloys, a long-sought capability critical for understanding alloy growth [25].

While energy-resolved maps of sample states can, in principle, be obtained by derivative spectroscopy [3], EF-STM introduces two key advances. It is inherently fast and simple and involves only constant-current imaging, so that it can be used to obtain spectroscopic information quickly or over large sample areas. And it is capable of mapping the three-dimensional structure of selected sample orbitals, whereas conventional derivative spectroscopy maps only the surface-projected "shape" of orbitals, providing no information on their extension into the vacuum.

Our experiments demonstrate the selective mapping of adatom and rest-atom orbitals on Si(111)-(7×7), and give evidence of the feasibility of energy-filtered scanning tunneling microscopy using cleaved InAs tips. Other semiconductor materials will have similar energy-filtering capability if gaps exist in their projected bulk band structure. The energy-filtering characteristics could thus be altered by choosing a different tip material. Ultimately, the band structure of semiconductor STM probes may be tailored to tune and optimize spectroscopic contrast, drawing from the broad repertoire of tools developed for semiconductor band-structure engineering, including alloying, carrier confinement, and elastic strain.

[1] G. Binnig et al., Phys. Rev. Lett. **49**, 57 (1982).

[2] J. K. Gimzewski and C. Joachim, Science **283**, 1683 (1999).

[3] R. J. Hamers, R. M. Tromp, and J. E. Demuth, Phys. Rev. Lett. **56**, 1972 (1986).

[4] B. C. Stipe, M. A. Rezaei, and W. Ho, Science **280**, 1732 (1998).

[5] R. Wolkow and P. Avouris, Phys. Rev. Lett. **60**, 1049 (1988).

[6] R. J. Hamers, in *Scanning Probe Microscopy and Spectroscopy: Theory, Techniques, and Applications*, edited by D. A. Bonnell (Wiley, New York, 2000).

[7] R. S. Becker et al., Phys. Rev. B **39**, 1633 (1989).

[8] Cleaved semiconductor (GaAs) STM tips were previously used for spin-polarized tunneling. See, G. Nunes, Jr. and N. M. Amer, Appl. Phys. Lett. **63**, 1851 (1993); M. W. J. Prins, R. Jansen, and H. van Kempen, Phys. Rev. B **53**, 8105 (1996).

[9] We used cross-sectional transmission electron microscopy (TEM) to characterize the shape of such InAs tips at mesoscopic length scales. Low magnification TEM images show flat {110} cleavage planes that extend over several hundred nanometers and intersect in a narrowly confined region, thus creating a well-defined tip. From high-resolution TEM micrographs, we determine an overall tip radius of about 20 Å (see [10]).

[10] See EPAPS Document No. E-PRLTAO-90-081314 for a movie of bias-dependent cc-STM images for bias values between -1.0 and -2.0 V. A direct link to this document may be found in the online article's HTML reference section. The document may also be reached via the EPAPS homepage (http://www.aip.org/pubservs/epaps. html) or from ftp.aip.org in the directory /epaps/. See the EPAPS homepage for more information.

[11] K. D. Brommer et al., Phys. Rev. Lett. **68**, 1355 (1992).

[12] K. Takayanagi et al., J. Vac. Sci. Technol. A **3**, 1502 (1985).

[13] Adatoms and rest atoms are observed in noncontact atomic force microscopy; see M. A. Lantz et al., Phys. Rev. Lett. **84**, 2642 (2000).

[14] An alternative pathway would be direct tunneling into a bulk state of the tip. Our conclusions would be the same in this scenario.

[15] P. Sutter et al., Surf. Sci.(to be published).

[16] While gaps in the projected density of states do occur in metals, the use of a polycrystalline metal tip may prevent such gaps from blocking tunneling. In addition, the metal most commonly used in STM tips, tungsten, appears to have no projected gaps within the accessible range of bias values [N. A. W. Holzwarth et al., Phys. Rev. B **48**, 12136 (1993)].

[17] J. Ihm, A. Zunger, and M. L. Cohen, J. Phys. C **12**, 4409 (1979).

[18] The basis set includes plane waves with energies up to 50 Ry, and the Brillouin zone is sampled using ten special k points [19]. Nonlocal pseudopotentials are generated via the method of Troullier and Martins [20], and core correction [21] is used for In. The calculation suffers from the well-known band-gap underestimation common to all local-density-functional calculations [22]. The required corrections tend to have small k dependence, so that a rigid upward shift of the conduction-band energies yields a reasonable approximation to the correct band structure [22]. We have corrected our conduction bands in this way, so that the band gap matches the experimentally observed value of 0.418 eV [23].

[19] S. Froyen, Phys. Rev. B **39**, 3168 (1989).

[20] N. Troullier and J. L. Martins, Phys. Rev. B **43**, 1993 (1991).

[21] S. G. Louie, S. Froyen, and M. L. Cohen, Phys. Rev. B **26**, 1738 (1982).

[22] X. Zhu and S. G. Louie, Phys. Rev. B **43**, 14142 (1991).

[23] *Landolt Börnstein Numerical Data and Functional Relationships in Science and Technology* (Springer, Berlin, 1982), Vol. 17a.

[24] R. Wiesendanger, *Scanning Probe Microscopy and Spectroscopy: Methods and Applications* (Cambridge University Press, Cambridge, England, 1994).

[25] P. Venezuela and J. Tersoff, Phys. Rev. B **58**, 10871 (1998).